NANJING INSTITUTE OF GEOPHYSICAL PROSPECTING AND INSTITUTE OF PHYSICS PUBLISHING JOURNAL OF GEOPHYSICS AND ENGINEERING
J. Geophys. Eng. **1** (2004) 46–50 PII: S1742-2132(04)73757-7

Recovery of a target reflection underneath coal seams

Jian Guo[1] **and Yanghua Wang**[2]

[1] Nanjing Institute of Geophysical Prospecting, Weigang 21, Nanjing 210014, China
[2] Centre for Reservoir Geophysics, Department of Earth Science and Engineering, Imperial College London, London SW7 2AZ, UK

E-mail: guojian@igp.cn and yanghua.wang@imperial.ac.uk

Received 1 September 2003
Accepted for publication 10 November 2003
Published 11 February 2004
Online at stacks.iop.org/JGE/1/46 (DOI: 10.1088/1742-2132/1/1/005)

Abstract
This paper presents a strategy to recover a target seismic reflection of a potential gas reservoir immediately underneath a group of coal seams. First, a random noise attenuation technique, which is amplitude preserving, is applied to a stack section with usual low signal-to-noise ratio. Then, a stabilized inverse Q filtering technique is applied to correct for both phase and amplitude effects simultaneously. The latter can recover all the high-frequency components that are in principle recoverable and intelligently limit the attempt to compensate a given high-frequency wave component when its amplitude is attenuated to a level below the ambient noise level. As a consequence, the seismic bandwidth is increased and thereby the vertical resolution is enhanced so that the weak reflection of the target gas layer underneath the strong coal-seam reflections is clearly presented.

Keywords: random noise attenuation, inverse Q filtering, seismic resolution, gas reservoir, coal seams

1. Introduction

This paper presents a case study on seismic data processing. In the study area, reflection seismic surveys are often complicated by high-velocity layers that lie above deeper interfaces of interest. High-velocity hard layers sandwiching softer coal seams form a group of strong reflections, an effective cement interface that prevents the energy from penetrating the deeper layers. Thus, deeper reflections are commonly very weak in this area.

In addition, seismic data are generally observed to lose high frequencies with increasing travel time. The loss of high frequencies lengthens the dominant signal wavelength and thereby degrades the seismic resolution in general cases. In this particular area, the layer of interest, a potential gas-reservoir formation, is very close to the strong-reflection layers. Therefore, the weak reflection of interest is completely obscured by the lengthened wavelet of strong reflections on the top.

In this paper, we present a two-step strategy in the data processing stage to recover the target reflection of a potential gas layer immediately underneath a group of high-velocity layers. First, we use a random noise attenuation technique (Wang 1999) which is amplitude preserving to improve the signal-to-noise ratio (S/N) prior to further processing. Then we adopt a stabilized inverse Q filtering technique (Wang 2002) that can compensate for both phase and amplitude effects simultaneously, without boosting the ambient noise. The result is superior, as the amplitudes of the more high-frequency components have been compensated. The method recovers all the frequency components that are in principle recoverable, and intelligently limits the attempt to compensate a given high-frequency wave component when its amplitude has been attenuated to a level below the ambient noise level.

2. Random noise attenuation

Figure 1 is an example section of land seismic data with a relatively low signal-to-noise ratio. When an inverse Q filter is applied to real seismic data, high-frequency noise is also amplified since the amplitude compensation operator is an exponential function of the frequency. Thus, random noise attenuation should be performed prior to inverse Q filtering.

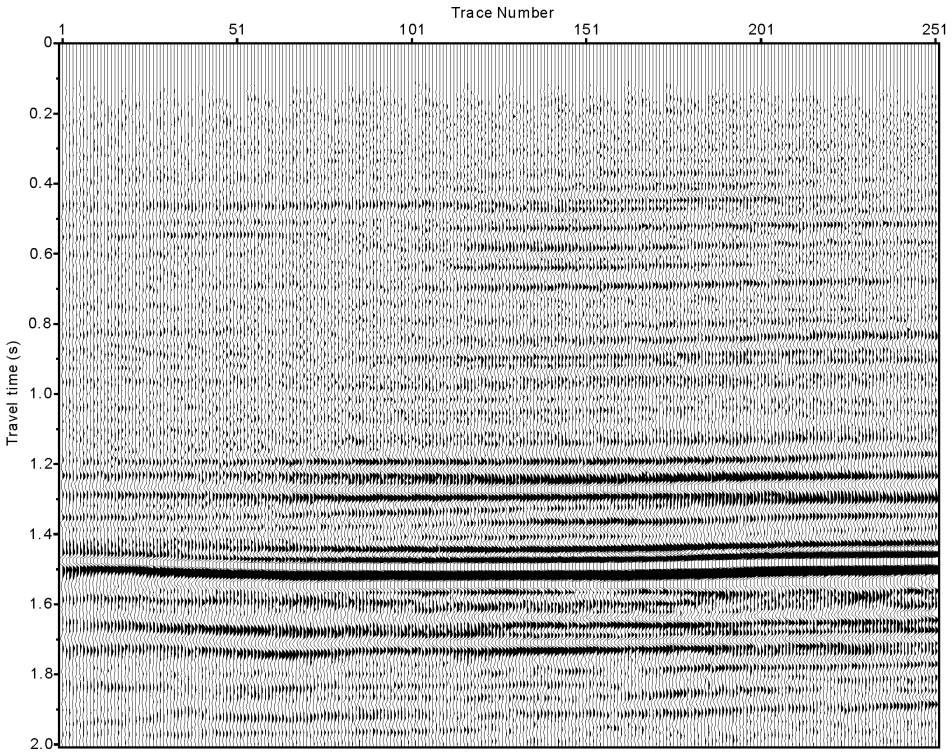

Figure 1. A sample stack section on which a potential target reflection immediately underneath the group of strong reflections at 1.5 s is not visible.

The random noise attenuation (RANNA) is commonly performed using the spatial linear prediction theory. It consists of two steps: estimating the linear prediction operator and applying it to filter seismic data. It is assumed that seismic signals in 2D data, for example, can be decomposed into different plane waves with different dips, which are predictable in the f–x domain. Once the prediction operator is obtained, the noise reduction filter is created and used to reconstruct a noise-free trace, for each frequency, as a weighted sum of its neighbouring traces at the corresponding frequency. This second step (i.e. filtering) can be understood to be parallel to a deconvolution procedure implemented in the Fourier transform space and, therefore, is conventionally referred to as FX-decon (Canales 1984, Gulunay 1986).

A RANNA algorithm using forward–backward linear prediction (FBLP) is presented in Wang (1999). The key step for RANNA is its first step, i.e. how to estimate the prediction operator for each frequency. It minimizes prediction residues in both forward and backward directions, instead of the forward prediction in a conventional FX-decon. In the second step, the two-side filter in a conventional FX-decon is built by flipping over the one-sided prediction operator, while the two-side filter in Wang (1999) is estimated directly from FBLP.

In a conventional FX-decon, the prediction operator is solved using a Levinson recursion algorithm, utilizing the property of the Toeplitz structure of the correlation matrix obtained from a Yule–Walker estimate. This estimate is asymptotically unbiased and always robust but, compared to estimators such as the ones that result from Burg's approach or from the one suggested in Wang (1999), of lower resolution. In addition, in order to keep the correction matrix in the Toeplitz form, zero-trace padding is required outside the design gate and causes errors, as those that are zero-trace are assumed implicitly to be 'alive' and contribute to the operator design. Those errors are called transient errors (Ulrych and Clayton 1976, Bunch and White 1985). This problem, inherent in the FX-decon, is overcome in the FBLP version of RANNA by using a transient-free formulation (without zero-trace padding), which calculates the operator only where non-zero data are available.

Figure 2 is the section after random noise attenuation. The amplitudes of both strong and weak coherent events have been preserved successfully. Figure 3 displays removed noise, i.e. the difference between the sections shown in figures 1 and 2. It visually verifies that the energy attenuated is really behaving randomly. Those noise traces in figure 3 could be mixed back to the resultant section of inverse Q filtering on the noise-suppressed traces.

3. Inverse Q filtering

Inverse Q filtering is then performed using a stabilized algorithm that can compensate for both phase and amplitude effects simultaneously, without boosting the ambient noise.

Given $U(0, \omega)$, the frequency-domain seismic trace recorded at surface ($\tau = 0$), the time-domain seismic signal after inverse Q filtering is denoted $u(\tau)$. Stabilized inverse

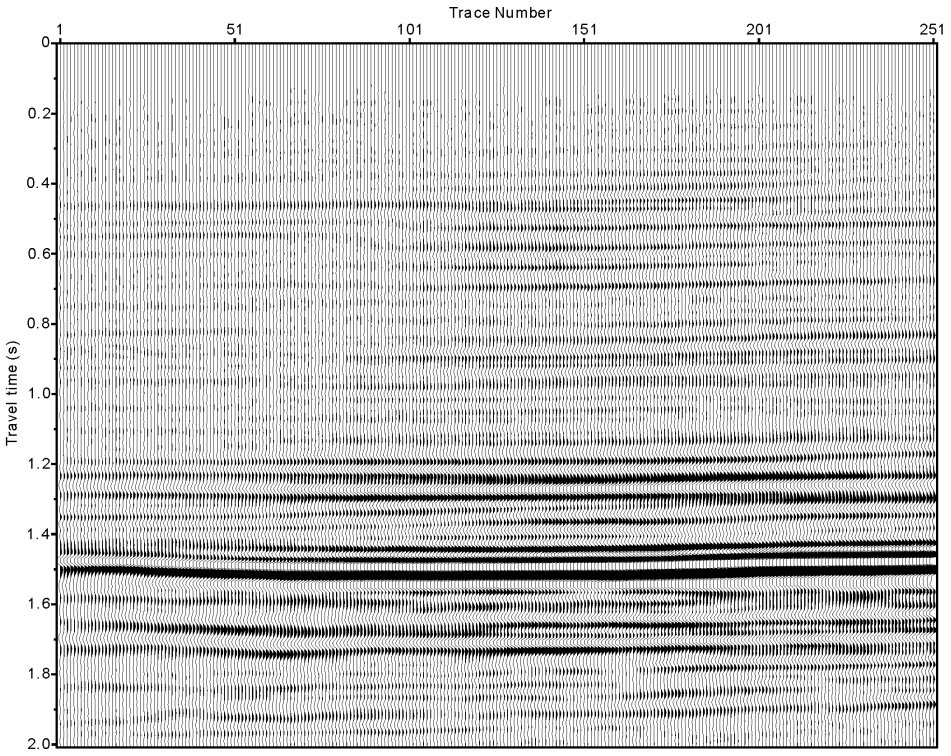

Figure 2. The stack section after random noise attenuation. The amplitudes of both strong and weak coherent events have been preserved successfully.

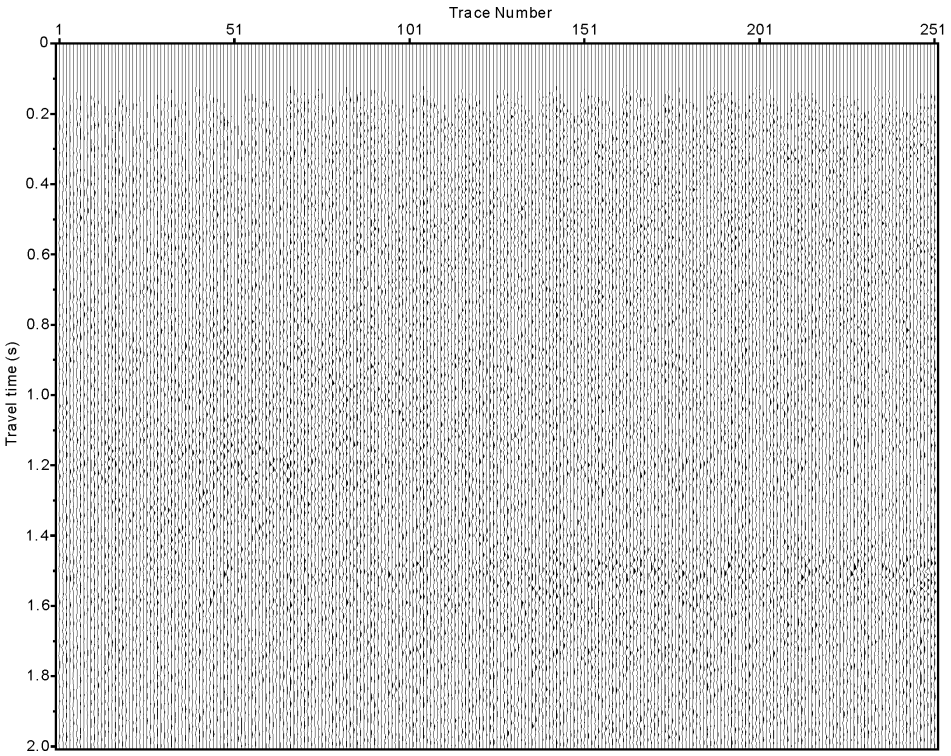

Figure 3. The noise removed by random noise attenuation. This visually verifies that the energy attenuated is really the random noise.

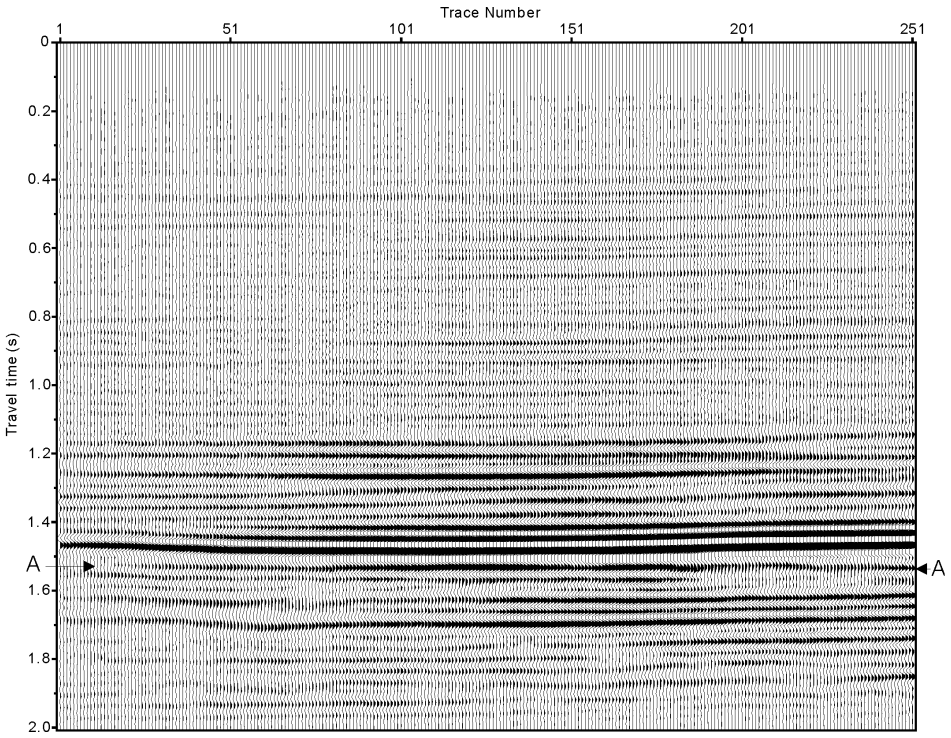

Figure 4. Seismic section after inverse Q filtering. It has successfully recovered the reflection 'A-A' of the potential gas reservoir (about 1.52–1.56 s), which is immediately underneath a group of strong coal-seam reflections.

Q filtering may be expressed as

$$u(\tau) = \frac{1}{\pi}\int_0^\infty U(0,\omega)\Lambda(\tau,\omega) \times \exp\left[\mathrm{i}\int_0^\tau \left(\frac{\omega}{\omega_\mathrm{h}}\right)^{-\gamma(\tau')}\omega\,\mathrm{d}\tau'\right]\mathrm{d}\omega, \quad (1)$$

where $\Lambda(\tau,\ \omega)$ is a stabilized amplitude compensation operator, $\gamma(\tau)$ is a time-variant attenuation parameter, $\gamma(\tau) = [\pi Q(\tau)]^{-1}$, and ω_h is a reference frequency (Wang 2002).

Stabilized inverse Q filtering, equation (1), must be performed successively on each time sample τ. Therefore, it may be rewritten in discrete form as

$$\begin{bmatrix} u_0 \\ u_1 \\ \vdots \\ u_M \end{bmatrix} = \begin{bmatrix} a_{0,0} & a_{0,1} & \cdots & a_{0,N} \\ a_{1,0} & a_{1,1} & \cdots & a_{1,N} \\ \vdots & \vdots & & \vdots \\ a_{M,0} & a_{M,1} & \cdots & a_{M,N} \end{bmatrix} \begin{bmatrix} U_0 \\ U_1 \\ \vdots \\ U_N \end{bmatrix}, \quad (2)$$

or presented in a vector-matrix form as

$$\mathbf{x} = \mathbf{A}\mathbf{z}, \quad (3)$$

where $\mathbf{x} = \{u(\tau_i)\}$ is the time-domain output data vector, $\mathbf{z} = \{U(\omega_j)\}$ is the frequency-domain input data vector, and $\mathbf{A}$ $(M \times N)$ is the inverse Q filter with an element defined as

$$a_{i,j} = \frac{1}{N}\Lambda(\tau_i,\omega_j)\exp\left[\mathrm{i}\int_0^{\tau_i}\left(\frac{\omega_j}{\omega_\mathrm{h}}\right)^{-\gamma(\tau')}\omega_j\,\mathrm{d}\tau'\right], \quad (4)$$

in which $\Lambda(\tau_i,\ \omega_j)$ is the stabilized amplitude compensation operator, and the exponential term is the phase correction term of inverse Q filtering. As the operators for amplitude compensation and phase correction vary with τ, this inverse Q filtering algorithm is applicable to a Q model varying with time or depth.

Figure 4 is the result of inverse Q filtering on the noise-attenuated section (figure 2). In this example, we estimate Q values from the stack section and then use them for inverse Q filtering. The interval Q values are listed as follows:

time(s)	0.1–1.0	1.0–1.3	1.3–1.6	1.6–2.0
Q	39.5	48.9	98.9	153.8

Note that in the plot of figures 1–3, a time-squared gain recovery has been applied in order to boost the weak amplitudes for an easy visual comparison to the inverse Q filtered result shown in figure 4. Comparing figure 4 with figures 1 and 2, we can make the following observations.

(1) The resolution has improved because of the larger frequency bandwidth, typically in the deep portion, and the high S/N ratio. Wang (2003) proposed a mathematic formula that shows resolution improvement is not only a function of the bandwidth change but also a function of the S/N enhancement.
(2) More coherent events have appeared underneath the group of strong reflections at 1.5 s. Any improvement in continuity of the events in figure 4 should be reliable because the inverse Q filtering algorithm works purely trace by trace (i.e. it is not a multi-channel process).
(3) In figure 4, immediately underneath the group of strong reflections, the target reflection 'A-A' (at time 1.52–1.56 s) has been recovered. It was destroyed because

of the phase distortion of the group of strong reflections and now stands out clearly after a proper phase correction.

The example section is arbitrarily selected from a 3D seismic cube. We would expect that if inverse Q filtering were applied to the whole 3D stack database, it would enhance the 3D migration process, which would benefit from the higher bandwidth.

4. Conclusions

In this paper, we have presented a strategy for recovering a target reflection of a potential gas reservoir immediately underneath a group of coal seams. We have used a random noise attenuation technique, which is amplitude preserving, and then a stabilized inverse Q filtering technique that can compensate for both phase and amplitude effects simultaneously, without boosting the ambient noise.

The result is superior, as the S/N ratio has been improved and the amplitudes of more high-frequency components have been compensated. It has recovered all the frequency components that are in principle recoverable, and intelligently limited the attempt to compensate a given high-frequency wave component when its amplitude has been attenuated to a level below the ambient noise level. As a consequence, the frequency bandwidth is increased, and thereby the vertical resolution is enhanced so that the weak reflection of the target gas layer underneath the strong coal-seam reflections is clearly presented.

References

Bunch A W H and White R E 1985 Least-squares filtering without transient errors: an examination of the errors in the least-squares filter design *Geophys. Prospect.* **33** 657–73

Canales L L 1984 Random noise reduction *54th SEG Meeting (Atlanta, USA)* Expanded Abstracts pp 525–7

Gulunay N 1986 FXDECON and complex Wiener prediction filter *56th SEG Meeting (Houston, USA)* Expanded Abstracts pp 279–81

Ulrych T J and Clayton R W 1976 Time series modelling and maximum entropy *Phys. Earth Planet. Inter.* **12** 188–200

Wang Y 1999 Random noise attenuation using forward-backward linear prediction *J. Seism. Explor.* **8** 133–42

Wang Y 2002 A stable and efficient approach to inverse Q filtering *Geophysics* **67** 657–63

Wang Y 2003 Quantifying the effectiveness of stabilized inverse Q filtering *Geophysics* **68** 337–45